Journal of Molecular Liquids 329 (2021) 115555

Contents lists available at ScienceDirect

Journal of Molecular Liquids

journal homepage: www.elsevier.com/locate/molliq

$Tb_2(WO_4)_3$@N-GQDs-FA as an efficient nanocatalyst for the efficient synthesis of β-aminoalcohols in aqueous solution

Sajjad Azizi [a,1], Mahdieh Darroudi [b,1], Jafar Soleymani [a], Nasrin Shadjou [c,*]

[a] Pharmaceutical Analysis Research Center, Tabriz University of Medical Science, Tabriz, Iran
[b] Department of Energy Science and Technology, Faculty of Science, Turkish- German University, 10634820 Istanbul, Turkey
[c] Department of Nanotechnology, Faculty of Science and Chemistry, Urmia University, Urmia, Iran

ARTICLE INFO

Article history:
Received 9 January 2021
Received in revised form 28 January 2021
Accepted 30 January 2021
Available online 2 February 2021

Keywords:
Tungstate nanoparticles, graphene quantum dots
Heterogeneous catalysis
Folic acid
β-Aminoalcohols

ABSTRACT

In the current study, $Tb_2(WO_4)_3$@N-(GQDs) modified with folic acid (FA) was synthesized during the chemical reaction of terbium (III) tungstate nanoparticles with nitrogen doped graphene quantum dots (N-GQDs) and introduced as a heterogeneous catalyst for the synthesis of β-aminoalcohols derivatives. The as-prepared $Tb_2(WO_4)_3$@N-GQDs-FA is stable at −4 °C for at least two month. Herein, the reaction time, solvent, and catalyst amount were optimized. The Tb nanostructure exhibited a high efficiency, less reaction time, excellent selectivity, and simple procedure for these transformations. The performance $Tb_2(WO_4)_3$@N-GQDs-FA nanocatalyst catalyst is thoroughly investigated which shows several advantageous including to facile preparation from readily available materials. Shorter reaction times, easy work-up, green reaction media, higher yields (near 97%), and no need to use the chromatographic column are the advantages of the reported synthetic method. The $Tb_2(WO_4)_3$@N-GQDs-FA heterogeneous catalyst has been recovered through filtration and also reused for multiple cycles. The recovered catalyst can be used for another nine successive reaction without noticeable loss in activity. The reaction time is also reduced and products can be obtained by convenient workup, and environmental-friendly procedure.

1. Introduction

β-aminoalcohols are ubiquitous in pharmaceutical molecules and natural products. The development of methods for the preparation of aminoalcohol scaffolds as a biologically active compound is a significant endeavor in the field of organic chemistry [1–6]. However, the reactivity of this disubstituted structure could be challenging since this 1,2-dipolar substitution relationship between amino and hydroxyl groups create a dissonant pattern about C skeleton [7,8]. The prevalence of this moiety has spurred the catalyst development for β-aminoalcohols preparation, which nucleophilic opening of aziridine and epoxide rings, and the aminohydroxylation of alkene and are the most advanced procedures [9–25]. As a result, considerable attention to develop environmental and viable routes to syntheisiz aziridine or epoxide rings' ring-opening have been developed [26]. The aminolysis procedure in the absence of a catalyst could be considered as a favored method in some cases; however, it also has some demerits as prolonged reaction time or high temperature [27,28]. Otherwise, the aminolysis reaction in the presence of different catalytic system was reported to overwhelm these limitations, such as $Zn(OTf)_2$ [29], $LiBF_4$, $CaCl_2$ [30], $[i\text{-PrO}]_2AlOOCCF_3$ [31], $CoCL_2$ [30], $Bi(OTf)_3$ [32] and LiOTF [32] under microwave radiation, alumina [33], silica under high pressure [34], SBA modified by Fe(III) salen [35] have been implemented to make important advances in regioselectivity, reaction time, temperature, environmentally friendly condition. Thus, developing an efficient catalytic protocol for epoxide ring-opening under ambient temperature is necessary.

Nanomaterials, due to their unique electrical and optical properties and also large surface to volume ratio, have been subjects of different field of study. To date, remarkable progress has been made in developing novel nanocatalysts [36–44]. Quantum dots (QDs) are one of the extensively researched nanoparticle systems. The synthesis of graphene quantum dots (GQD) has become a popular topic in recent years [45–52]. The term GQD is usually used to describe miniscule fragments, limited in domains or size of single-layer to tens of layers of graphene. GQD often possess unique properties like optical, stable photoluminescence, pronounced quantum confinement effect, which makes them attractive for energy, optoelectronic, catalytic, biological, and environmental applications [50–53]. While graphene usually does not have a bandgap, GQD contains a bandgap due to edge effects and quantum confinement. The bandgaps modify graphene's carrier

---

[*] Corresponding author.
E-mail address: n.shadjou@urmia.ac.ir (N. Shadjou).
[1] Equal contribution and co-first author.

https://doi.org/10.1016/j.molliq.2021.115555

behavior and may lead to different applications. GQD was also found to have four quantum states at given energy levels, unlike semiconductor QD, which has just two [54–61]. According to previous reports, these additional quantum states could make GQDs beneficial for quantum computing. The GQD has a large surface and mostly contains a rich surface of functional groups on carbon [61,62]. The richest functional groups are carboxylic groups and amine groups, which can be electron acceptor and donor, and thus can be instantly conjugated to ions (terbium GQD). Terbium is an essential rare earth element that has a very low concentration in the earth's crust [45,63–65]. Its unique electronic layout state determines its critical application in color television, optical actuators, catalysis, and the fluorescence lamp.

β-aminoalcohols has been used extensively in the synthesis of therapeutic due to its structural similarity to neurotransmitters and hormones [66–69]. We aimed to produce β-aminoalcohols regioselectively through utilize unexplored opening of styrene oxide and aniline [9,18]. Herein, we have prepared $Tb_2(WO_4)_3$@N-GQDs-FA nanocatalyst, and also characterization, the ability of terbium tungstate functionalized with a GQD matrix was investigated in the catalytic performance in order to the synthesis of β-aminoalcohols under mild and green conditions at room temperature. $Tb_2(WO_4)_3$@N-GQDs-FA shows a yield of 97% for the preparation of β-aminoalcohols (with wt% catalyst loading). The catalytic activities of nanocatalyst are further improved.

2. Experimental

2.1. Methods and materials

All the commercial-grade chemicals and reagents were used without further purifications purchasing from Merck Company. The reaction was monitored using analytical thin-layer chromatography (TLC) with ethyl acetate/n-hexan as eluents. Due to the need to achieve final pure and isolated target molecules, a scaled-up TLC was used. The definite characterization of all products was done with ^{1}H NMR (500 MHz) and ^{13}C NMR (125 MHz) spectra recorded with a Bruker DRX-500 Avance spectrometer using DMSO-$d_6$as a solvent at ambient temperature. All yields referred to isolated products. The Infrared spectra (IR) of the sample were recorded from KBr disc by Fourier-Transform (FT-IR) Shimadzu FT-IR-8400S spectrometer in the range of 500 to 4000 cm^{-1}. The transmission electron microscopy (TEM) images were obtained by a Carl Zeiss LEO 906 electron microscope operated at 100 kV (Oberkochen, Germany). The Zeta potential of GQD GQD-Tb was measured by ZETASZER ZS90. The UV–Vis spectrometer was performed using Shimadzu UV 3600 spectrometer. Fluorescence spectra were analyzed by a Jasco FP 750 spectrophotometer (Tokyo, Japan).

2.2. Synthesis of nanomaterials

2.2.1. Preparation of $Tb_2(WO_4)_3$ NPs

The terbium (III) tungstate nanoparticles were synthesized according to an optimized process which was previously reported by Rahimi et al. [7,8]. Generally, 0.01 M terbium ion (Tb^{3+}) was added over to the tungsten ion solution (0.005 M) and then stirred. After that, the white solid was filtered and washed several times with absolute ethanol and water. Finally, as prepared participated was dried at 80 °C for at least 4 h.

2.2.2. Preparation of $Tb_2(WO_4)_3$@N-GQDs nanocomposite

$Tb_2(WO_4)_3$@N-GQDs was synthesized according to following method. 1 g of citric acid and 0.4 mL of ethylenediamine was added into 15 mL water and stirred to dissolve. Then, 50 mg of as-prepared $Tb_2(WO_4)_3$ NPs were added to the mixture. Next, the mixture was transferred into a 50-mL Teflon-lined stainless hydrothermal synthesis autoclave and heated to 180 °C and kept for about 8 h. Afterward, the mixture was cooled to room temperature. Finally, as-synthesized nanomaterials were centrifuged (10.000 rpm for 15 min) to remove solid particles. The obtained $Tb_2(WO_4)_3$@N-GQDs was dialyzed possible unreacted materials.

2.2.3. Preparation of NHS-FA

FA-NHS was prepared according to the EDC/NHS reaction. In brief, 60 mg of FA, 12 mg of NHS, and 10 mg of EDC were dissolved in about 12 mL of DMSO-d6, and then 150 μL of TEA was added and agitated at room temperature for about 18 h. Subsequently, TEA molecules were evaporated using a vacuum. Finally, the produced FA-NHS was kept at −4 °C for the next uses.

2.2.4. Preparation of $Tb_2(WO_4)_3$@N-GQDs-FA

20 mL of $Tb_2(WO_4)_3$@N-GQDs solution was added to the 12 mL of the NHS-FA solution and stirred at room temperatures for about 3 h. Finally, $Tb_2(WO_4)_3$@N-GQDs-FA black-brown solution was centrifuged and dialyzed (3000 Da) toward deionized-waste for at least 3 days. The as-prepared $Tb_2(WO_4)_3$@N-GQDs-FA is stable at −4 °C for at least two months.

2.3. General procedure for syntheis of β-Aminoalcohols

To investigate the catalytic performance of the $Tb_2(WO_4)_3$@N-GQDs-FA catalyst toward β-aminoalcohols preparation, styrene oxide and aniline was chosen as the test substrates. The optimization of the reaction conditions of styrene oxide and aniline in the presence of $Tb_2(WO_4)_3$@N-GQDs-FA in different conditions are summarized in Table 2. The reaction mixture was monitored by TLC. After completion of the reaction, the $Tb_2(WO_4)_3$@N-GQDs-FA catalyst was separated through centrifuging and the residue was purified from the reaction mixture by silica plate. To clarify the scope and restrictions of the $Tb_2(WO_4)_3$@N-GQDs-FA catalytic system in reaction with styrene oxide, under carefully optimized reaction condition, various aromatic and aliphatic amines were examined (Table 1). The ring-opening reaction was found to be fast, and nearly completion of conversion was obtained within 30 min, which led to the quantitative β-aminoalcohols yield.

Table 1
Optimization of β-Aminoalcohol preparation.

Entry	Catalyst (mg)	Time (min)	Solvent	Temperature (°C)	Yield, %
1	10	30	Water	r.t	60
2	10	30	Solvent-free	r.t	10
3	10	30	MeOH	r.t	71
4	10	30	Acetonitrile	r.t	5
5	10	30	Toluene	r.t	15
6	10	30	n-Hexane	r.t	**N**
7	10	30	EtOH	r.t	97
8	0	30	EtOH	r.t	0
9	1	30	EtOH	r.t	5
10	2.5	30	EtOH	r.t	33
11	5	30	EtOH	r.t	54
12	7.5	30	EtOH	r.t	79
13	20	30	EtOH	r.t	97
14	30	30	EtOH	r.t	97
15	40	30	EtOH	r.t	97
16	10	30	EtOH	r.t	97
17	10	30	EtOH	Reflux	97
18	10	0	EtOH	r.t	0
19	10	5	EtOH	r.t	10
20	10	10	EtOH	r.t	41
21	10	20	EtOH	r.t	67
22	10	30	EtOH	r.t	97
23	10	40	EtOH	r.t	97
24	10	50	EtOH	r.t	97
25	10	60	EtOH	r.t	97
26	10	70	EtOH	r.t	97

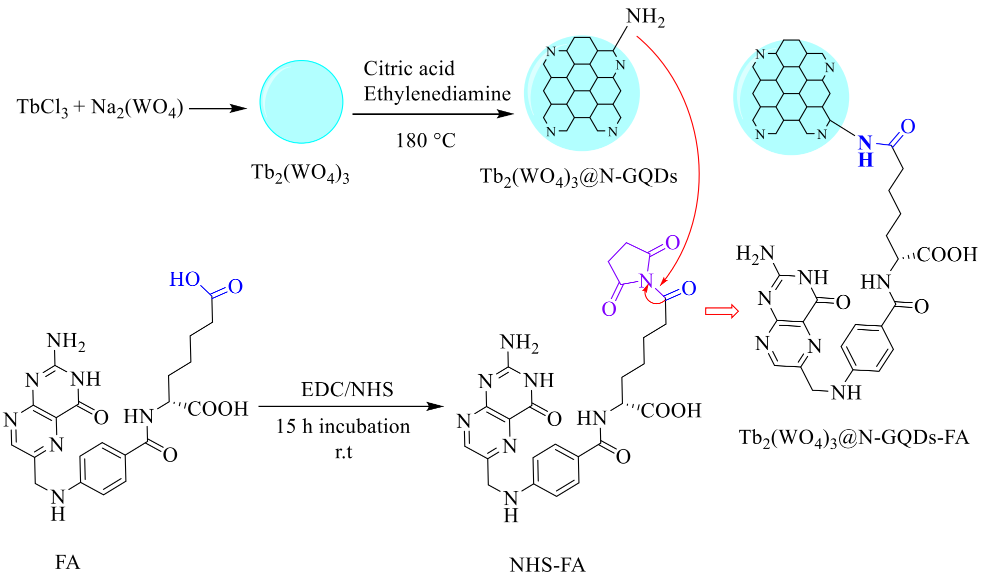

Scheme 1. Preparation of $Tb_2(WO_4)_3$@N-GQDs-FA

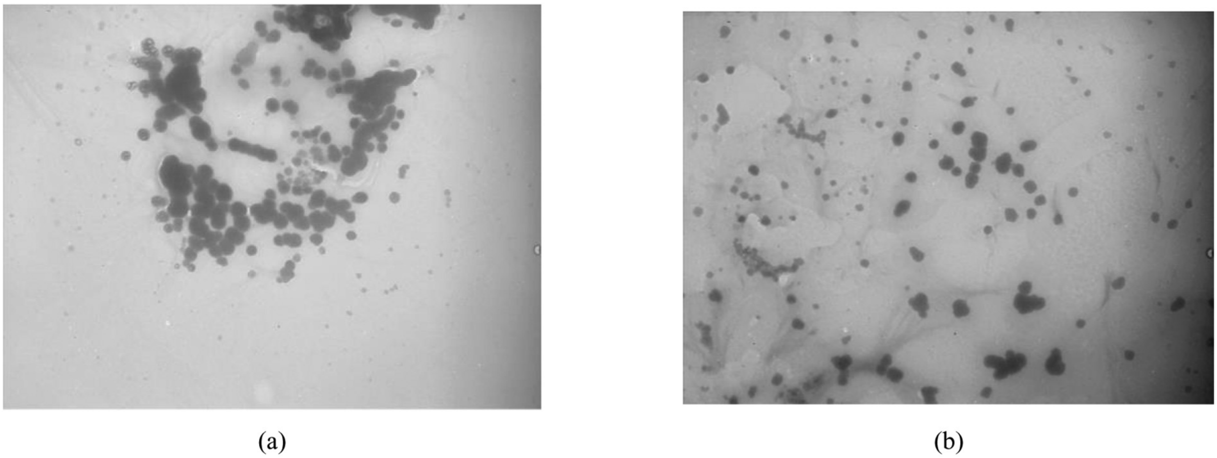

Fig. 1. TEM image of $Tb_2(WO_4)_3$@N-GQDs-FA in diferent magnification.

3. Results and discussion

3.1. Material characterization

The prepared GQD was simply synthesized through refluxing in the mixture of concentrated citric acid and EDTA at 180 °C in an oil bath. The synthetic method of the functionalized $Tb_2(WO_4)_3$@N-GQDs-FA has been illustrated in scheme 1. The TEM image of the prepared GQD is shown in Fig. 1. It revealed the morphology of functionalized GQD with an average size at 2–5 nm and a narrow size range at 4 nm. Also, the surface electron density was measured by the Zeta potential analyzer and demonstrated an average size at 0.90 nm (Fig. 2).

To determine functional groups, surface state, and composition of the $Tb_2(WO_4)_3$@N-GQDs-FA, the characterization was measured by the FT-IR. The FT-IR spectrum exhibited a broad absorption peak at 3330 cm^{-1}, which is attributed to the hydroxyl and N—H on the surface of the modified N-GQDs. In additions, two addorption peaks at 1551, and 1643 cm^{-1} belong to the stretching vibrations of the C═C and C═O bonds of N-GQDs, respectively and the peaks could be seen at the range of 680 and 540 cm^{-1} relating to Tb^{3+} bonds. Also, the peak around 1500 cm^{-1} is related to amide bonds between carboxyl of FA and amine group of $Tb_2(WO_4)_3$@N-GQDs. The zeta potential analysis of $Tb_2(WO_4)_3$@N-GQDs-FA nanocomposite was determined to check the influence of Tb ions, which doped on the surface charge and slow the exact doping of N-GQDs-FA nanocomposite with $Tb_2(WO_4)_3$ species. Thus, the nanomaterial exhibited a negative external charge, which confirmed the fixing FA and $Tb_2(WO_4)_3$ ion groups on the superficial spaces of the N-GQD composite (Fig. 3).

The scanning electron microscopy micrograph (SEM) was used to indicate the morphology of $Tb_2(WO_4)_3$@N-GQDs-FA, which exhibited the fibrous-like structure of catalyst (Fig. 4). The chemical composition of $Tb_2(WO_4)_3$@N-GQDs-FA nanocomposites was also studied through EDX analysis, which confirmed the presence of Tb and W in the catalyst along with the other elements, indicating the formation of the desired structure of nanocomposite. The loading Tb metal was found to be 0.018 mmol/g of the catalyst (0.02 wt%). As shown in Fig. 5, the EDX measurement confirmed that the nanocatalyst contains C, N, O, Na, Tb, and W.

3.2. Absorption properties

The optical properties of synthesized $Tb_2(WO_4)_3$@N-GQDs-FA and GQD solution using the UV–Vis absorption were studied (Fig. 6). The

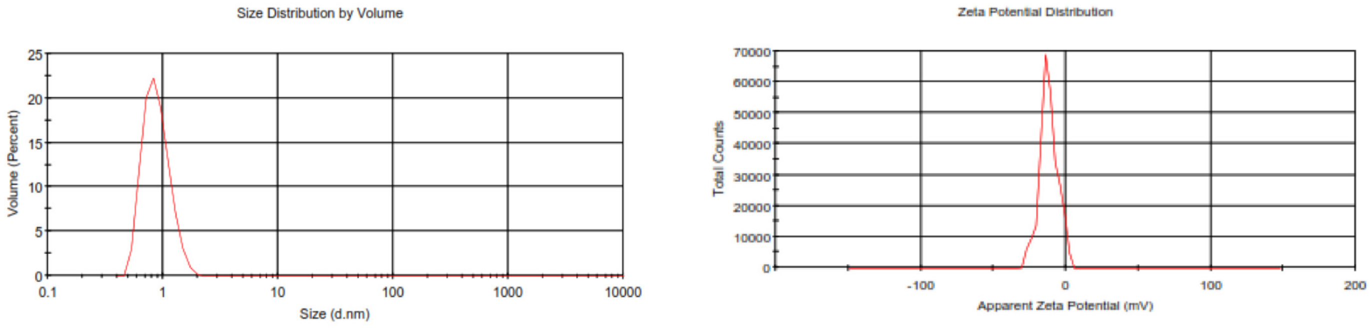

(a)

(b)

Fig. 2. FLS and Zeta potential analyzer $Tb_2(WO_4)_3$@N-GQDs-FA.

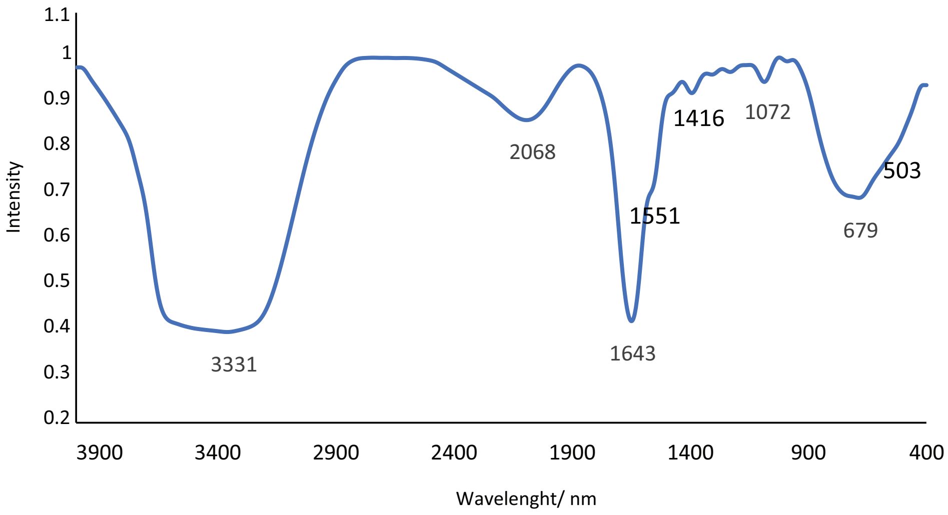

Fig. 3. The FT-IR spectum of $Tb_2(WO_4)_3$@N-GQDs-FA.

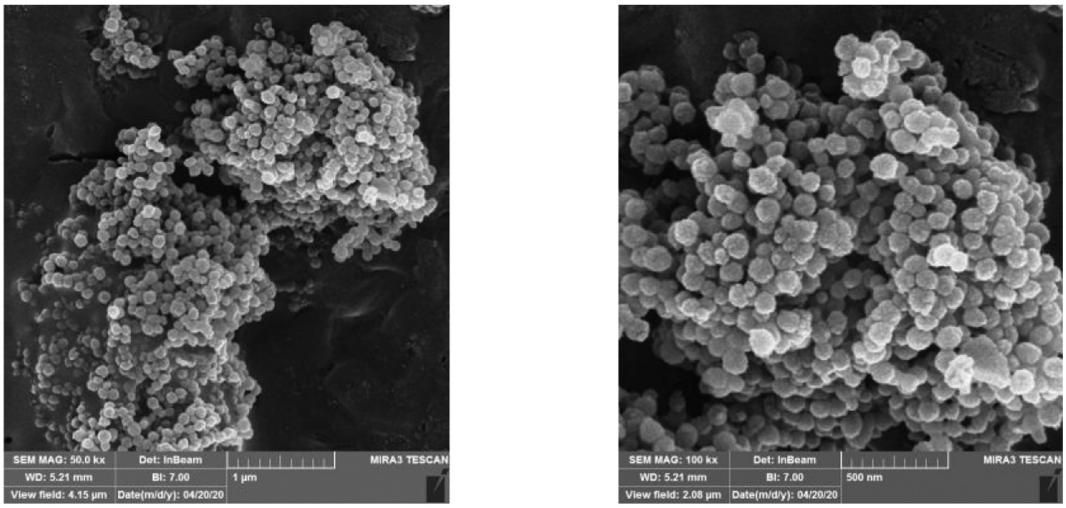

(a)

(b)

Fig. 4. SEM images of $Tb_2(WO_4)_3$@N-GQDs-FA nanocomposite in dfferent magnification.

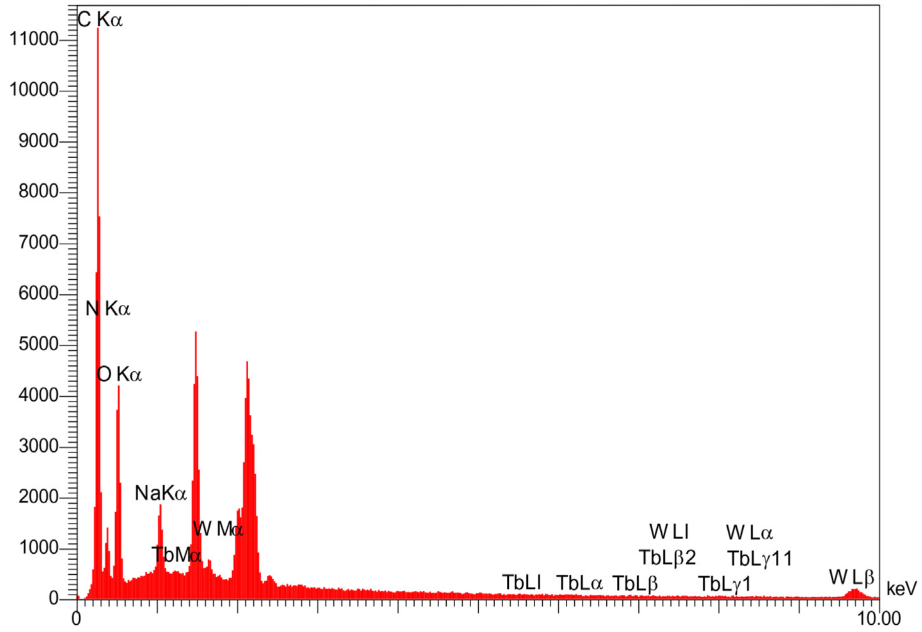

Fig. 5. EDX SEM images of $Tb_2(WO_4)_3$@N-GQDs-FA nanocomposite.

blue line represented the UV–Vis of $Tb_2(WO_4)_3$, the orange line presented UV–Vis absorption of $Tb_2(WO_4)_3$@N-GQDs, and the gray line, showed $Tb_2(WO_4)_3$@N-GQDs-FA. As shown in Fig. 5, the addition of $Tb_2(WO_4)_3$ in GQD altered the optical properties of the synthesized GQD. The UV–Vis spectra of $Tb_2(WO_4)_3$ demonstrated two characteristic peaks at 240 and 345 nm are attributing to π-π* and n-π* transition, which in addition to GQD, the absorbance intensity altered. As for the $Tb_2(WO_4)_3$@N-GQDs solution, both of the absorption peaks at 240 and 345 nm was found to decrease, which implied interaction between metal ions and GQD in the solution, likely the apparent affinity of metal ion to O atom of the donor group [35]. Furthermore, the absorption peak of $Tb_2(WO_4)_3$@N-GQDs-FA demonstrated absorption peaks at 258 and 286, and 372 nm, which have a clear blue shift by 25 nm, and the new absorption peak can be attributed to the $C{=}O$ bonded $Tb_2(WO_4)_3$ complex [36].

3.3. Fluorescence spectra

The fluorescence spectra of the $Tb_2(WO_4)_3$@N-GQDs-FA, $Tb_2(WO_4)_3$, N-GQDs, FA, and N-GQDs-FA are shown in Fig. 7. All the photoluminescence studies were performed in an aqueous medium. Upon excitation at 220 nm, the strong emission peaks are observed at 260, 330, 410, and 620 nm, which are ascribed to the intra configurational $^5D_4 \rightarrow {}^7F_6$, $^5D4 \rightarrow {}^7F_5$, $^5D_4 \rightarrow {}^7F_4$ and $^5D_4 \rightarrow {}^7F_3$ electron transmission for $Tb_2(WO_4)_3$, sequential [70,71]. Moreover, fluorescent spectra of the N-GQDs nanocomposite upon excitation 300 nm, exhibited a strong

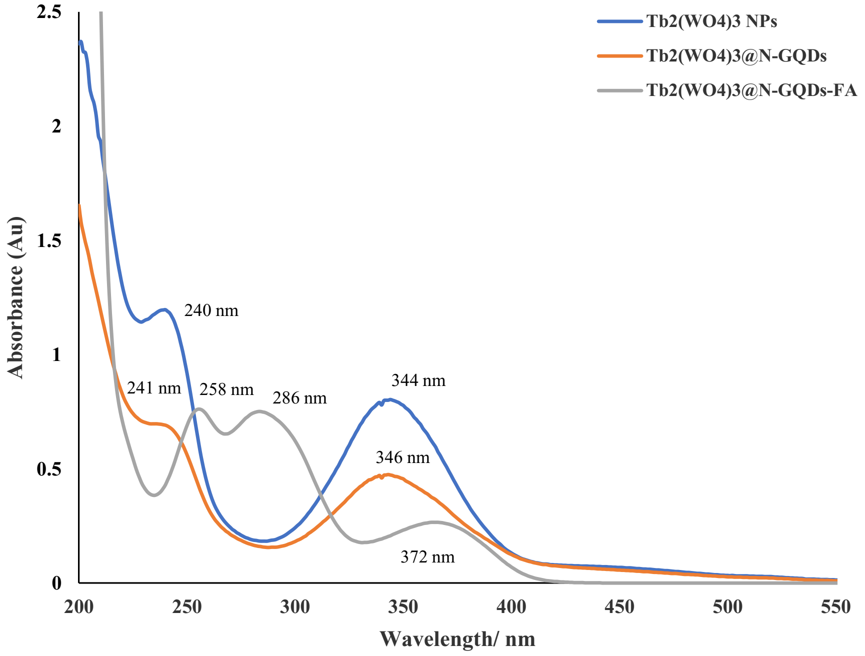

Fig. 6. The UV–Vis absorptions of $Tb_2(WO_4)_3$, $Tb_2(WO_4)_3$@N-GQDs, $Tb_2(WO_4)_3$@N-GQDs-FA.

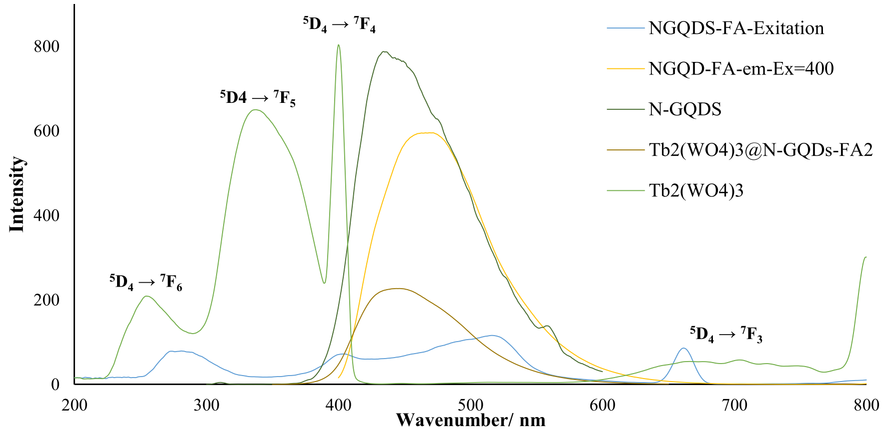

Fig. 7. Fluorescence spectra of $Tb_2(WO_4)_3$@N-GQDs-FA, $Tb_2(WO_4)_3$, N-GQDs, FA, and N-GQDs-FA.

peak at 435 nm and the N-GQDs-FA nanocomposite displayed a quenching peak at 435 nm efficacious preparation of nanocomposite. According to Fig. 7, $Tb_2(WO_4)_3$@N-GQDs-FA has some distinct emission peak, which is in agreement with the functionalized $Tb_2(WO_4)_3$@N-GQDs structure. Sp^2 hybridation and existence of oxygen-rich functional groups such as C—O, C═O and –COOH on the surface of N-GQDs are caused to the decline on the fluorescence emission.

3.4. Application of $Tb_2(WO_4)_3$@N-GQDs-FA for β-aminoalcohols preparation

Once the catalytic activity of $Tb_2(WO_4)_3$@N-GQDs-FA nanocatalyst had been evaluated as a catalyst for the β-aminoalcohols preparation. Initial experiments using styrene oxide and aniline were performed as a model reaction to optimize various parameters comprising solvent, temperature, time, and catalyst. The results are listed in Table 1.

In order to optimize the reaction condition, the effect of solvent was surveyed in Table 1, which exhibited among the different solvents, such as solvent-free, H_2O, EtOH, MeOH, CH_3CN, Toluene, and Hexane (Table 1, Entry 1–7) depicted that the green solvent EtOH had the highest yield in the shortest reaction time, while other solvents and mixed solvents yielded a lower amount of product even in longer reaction time. Therefore, at the outset, EtOH was chosen as a reaction medium, and the model reaction was explored in various amounts of catalyst. When the reaction was repeated in the presence of catalyst including 1, 2.5, 5, 7.5, 10, 20, 30, and 40 mg of $Tb_2(WO_4)_3$@N-GQDs-FA nanocatalyst, resulted in the isolation of the product in a yield of 5, 33, 54, 79 and for more amount of catalysts were 97%, respectively (Table 1, Entry 9–15). In the absence of a catalyst at room temperature, after 30 min, no product was obtained (Table 1, Entry 8). It is noticanle that, catalyst-free reaction condition led to decreasing the rate of reaction and a considerable amount of starting materials remain intact even after prolonged reaction time. Also, the optimal value of temperature was interpreted, which demonstrated that raising the temperature of reaction does not affect the yield of reactions. Notably, the yield of reaction was independent toward temperature as in reactions with variable temperature from room temperature to about 78 °C, in EtOH and when the time is raised (Table 1, Entry 0.16 and 17). The reaction proceeded rapidly, as exhibited, in different times 5, 10, 20, 30, 40, 50, 60, and 70 min, resulting in the isolation of the product in a yield of 10, 41, 67, and for all others 97%, respectively (Table 1, Entry 18–26). It is clear that the yield of reaction enhances till the time of reaction increased to 30 min, and the reaction was completed after 30 min at room temperature. Considering these results, the optimal conditions for the optimization of model reaction were appointed 10 mg of the $Tb_2(WO_4)_3$@N-GQDs-FA nanocatalyst at room temperature and in EtOH as a green solvent in 30 min.

Then, the optimized conditions were used for the synthesis of β-Aminoalcohol scaffolds (Scheme 2) using a series of amine (1 mmol) and different substituted of epoxide (1 mmol) in ethanol (3 mL) and in the presence of 10 mg $Tb_2(WO_4)_3$@N-GQDs-FA nanocatalyst. To investigate the substrate scope, generality, and utility of this catalytic system, the epoxide ring-opening reaction was examined under optimal reaction conditions. It can be seen that all products were obtained in high yields (Table 2). Various amines were examined as substrates in the optimized reaction condition. The observed catalytic changes have been related to electronic and steric effects. The withdrawing substituted of amines, besides steric hindrance, had less reactivity, whereas the electron donor substituted of amine promoted a high yield in the transformation (Table 2). Both aromatic and aliphatic epoxide, including those bearing functional groups as oxabicyclic heptane, ethyl oxirane, styrene oxide, and phenoxy methyl-oxirane, were able to undergo the corresponding β-aminoalcohols preparation. Also, the aliphatic and aromatic amines were used in the model reaction to study the effect of substrate on the reactivity of reaction, resulting in β-aminoalcohol products in good yields (Table 2, Entries 1–12). Under the optimized conditions, aromatic amines such as aniline all give both higher conversion and greater yields at room temperature within the reaction time. However, the aliphatic amines with electron-withdrawing groups reacted more smoothly (Table 2, Entry 5). Electron donating groups exhibits significant reactivity, and also reactions were completed even at a lower temperature and higher conversion. Moreover, the aromatic epoxide, which has electron-rich groups, increased the reactivity of the transformation, whereas the aliphatic groups led to much lower yields (Table 2, Entries 1,9,10).

The proposed mechanism for the synthesis of β-aminoalcohols in the presence of $Tb_2(WO_4)_3$@N-GQDs-FA nanocatalyst is shown in Scheme 3. This catalyst with having many polar functional groups can

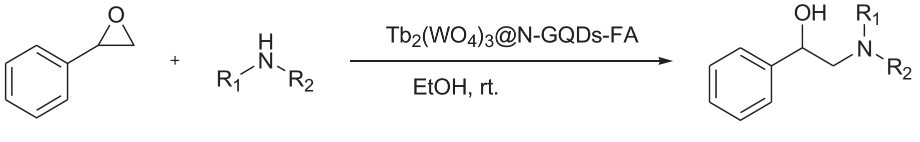

Scheme 2. Synthesis of β-aminoalcohols by $Tb_2(WO_4)_3$@N-GQDs-FA nanocatalyst

Table 2
Application of $Tb_2(WO_4)_3$@N-GQDs-FA nanocatalyst for synthesis of β-aminoalcohols under optimized reaction.

Entry	Amine	Oxirane	Yield
1	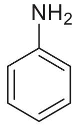	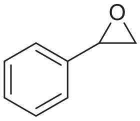	97
2	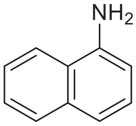	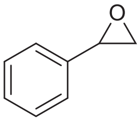	90
3	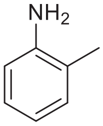	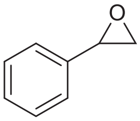	95
4	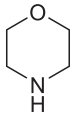	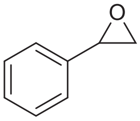	70
5	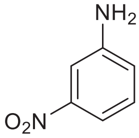	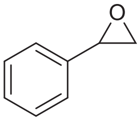	71
6	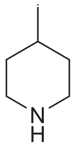	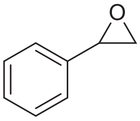	73
7	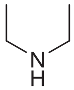	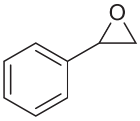	78
8	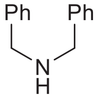	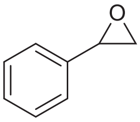	72
9	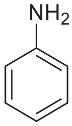	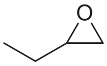	80
10	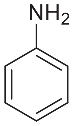	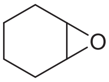	76
11	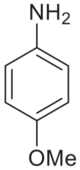	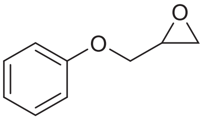	82
12	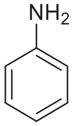	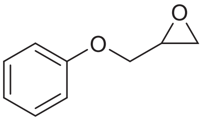	71

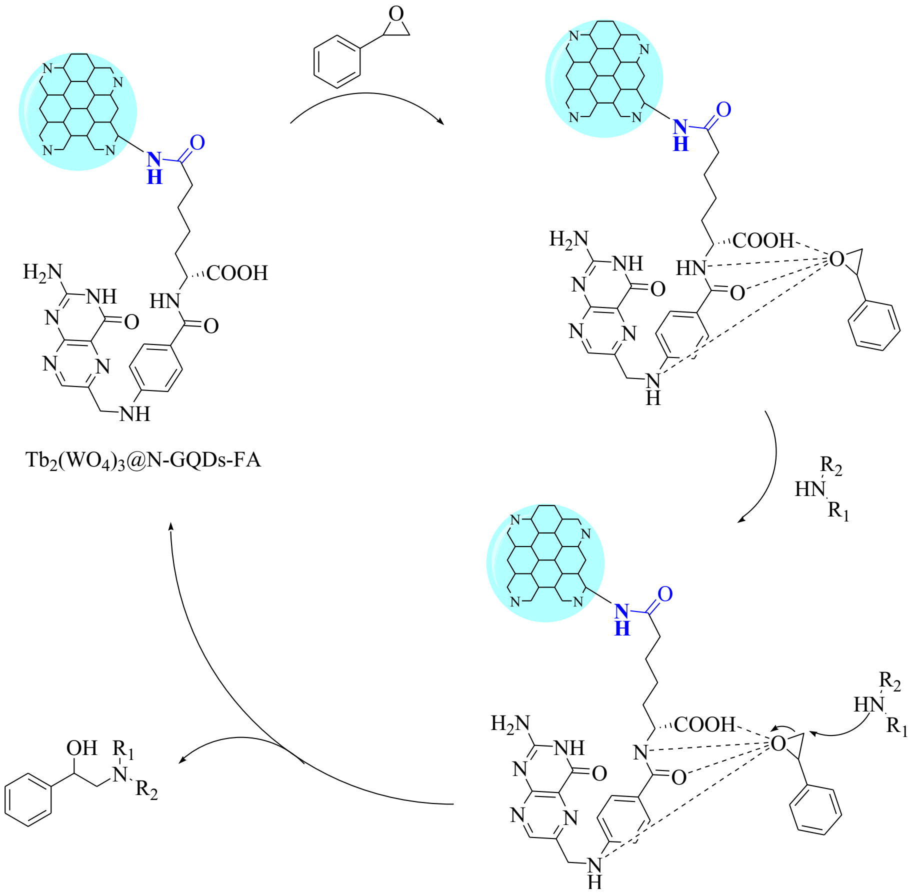

Scheme 3. Proposed mechanism for the synthesis of β-aminoalcohols in the presence of $Tb_2(WO_4)_3$@N-GQDs-FA nanocatalyst

easily activate a there membered epoxid ring through the hydrogen bonds interations. Then, by nucleophilic attacking of nitrogen atom in substituted amines to the activated epoxid ring, the high yield of products are obtained.

3.5. Recycling of the catalyst

One of the most crucial aspect of profitable heterogeneous catalysts is recyclability which make them attractive from economic point of view. In order to recover the $Tb_2(WO_4)_3$@N-GQDs-FA at reaction completion point, after the accomplishment of each cycle, according to aforementioned optimized reaction condition, the solid catalyst was separated simply by centrifugation followed by rinsing with ethanol (5 ml) for few times and at 50 °C. After drying through vacuum overnight and use again in a sequential run, the results exhibits that catalyst is substantially recyclable under the optimized reaction condition and even after nine times use, supported by analysis result provide in Fig. 8. Next, hot filtration test was applied to determine the stability characteristic of the $Tb_2(WO_4)_3$@N-GQDs-FA nanocatalyst. After 2 h, the reaction mixtures were centrifuged followed by filtration of catalyst. Then the supernatant was stirred at ambient temperature. Intriguingly, even after additional 4 h, there were not any considerable changes in the transformation reaction. Compared to previously recognized catalyst for aminolysis of epoxides, $Tb_2(WO_4)_3$@N-GQDs-FA is showing decent catalytic performance regarding to activity and recyclability (Table 3).

3.6. Performance of the catalyst

The performance of the prepared $Tb_2(WO_4)_3$@N-GQDs-FA nanoparticle, in comparison with the previously reported catalyst, is demonstrated in Table 3. Encouraged by this result, we subsequently examined various catalysts. Among different catalysts, $Tb_2(WO_4)_3$@N-GQDs-FA seemed to be the most active catalyst for the β-aminoalcohol preparation (Table 3, Entry 1–9). The use of other catalysts for this ring-opening reaction, such as nano $Fe(OH)_3$, $Fe_3O_4@SiO_2\text{-}SO_3H$, Al_2O_3, B-CD, LiBr, $Bi(OTf)_3$, Polymer/$CuSO_4$, Tb-MOF led to a lower yield of the reaction. Consequently, the proposed $Tb_2(WO_4)_3$@N-GQDs-FA nanocatalyst had some promising features, including stability, cost-effective method, less reaction time, and commercially available materials.

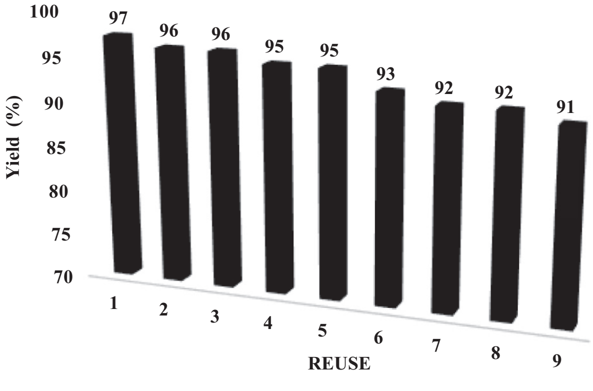

Fig. 8. Recyclability of the $Tb_2(WO_4)_3$@N-GQDs-FA nanoparticle in the aminolysis reaction of the epoxide.

Table 3
Assessment of the catalyst activity in comparison with previous work.

Entry	Catalyst	Amount (mg)	Temp	Solvent	Time (min)	Yield (%)
1	Nano Fe(OH)$_3$	20	RT	–	45	92
2	Fe_3O_4@SiO_2-SO_3H	10	RT	EtOH	180	82
3	Al_2O_3	6000	Reflux	THF	360	69
4	B-CD	–	60	Water	480	88
5	LiBr	5 mol%	RT	–	300	98
6	Bi(OTf)$_3$	0.05 mol %	Microwave	CH_3CN	33	96
7	Polymer/$CuSO_4$	–	RT	Cyclohexane	180	88
8	Tb-MOF	20	RT	EtOH	30	95
9	Tb$_2$(WO$_4$)$_3$@N-GQDs-FA	10	RT	EtOH	30	97

4. Conclusion

In summary, GQDs can act as a heterogeneous catalyst for a variety of organic reactions. We prepared a new Tb$_2$(WO$_4$)$_3$@N-GQDs-FA nanocatalyst and characterized by TEM, Zeta-DLS, SEM-EDX, IR, UV–Vis, and fluorescence. The efficiency of Tb$_2$(WO$_4$)$_3$@N-GQDs-FA nanocatalyst was examined in the synthesis of β-aminoalcohol analogs that have been successfully carried out through aminolysis of epoxides. This nanocatalyst was applied to prepare β-aminoalcohols under green and mild conditions at room temperature. In these reactions, a catalytic amount of heterogeneous catalyst is required which can be recovered to reuse after completion of reaction, simply by applying centrifugation. Shorter reaction times, easy work-up, green reaction media, higher yields (near 97%), and no need to use the chromatographic column are the advantages of the reported synthetic method. The recovered catalyst can be used for another nine successive reaction without noticeable loss in activity. The performance Tb$_2$(WO4)$_3$@N-GQDs-FA nanocatalyst catalyst is thoroughly investigated which shows several advantageous including to facile and low cost preparation from readily available materials. The reaction time is also reduced and products can be obtained by convenient workup, and environmental-friendly procedure.

Contribution

Sajjad Azizi: Methodology, Analysis data, Investigation, Writing-review and editing.

Mahdieh Darroudi: Analysis data, Writing Original draft and review and editing.

Jafar Soleymani: Investigation.

Nasrin Shadjou: Project administration, Investigation, Funding acquisition, Methodology, Supervision, Resources, Writing-review and editing.

Data Availability Statement

The data that support the findings of this study are available from the corresponding author upon reasonable request.

Declaration of Competing Interest

The authors declare no conflict of interest.

Acknowledgment

We gratefully acknowledge the financial support from Urmia University and Tabriz University of Medical Science.

References

[1] P. Gupta, N. Mahajan, New J. Chem. 42 (2018) 12296–12327.
[2] S. Wetzel, A. Schuffenhauer, S. Roggo, P. Ertl, H. Waldmann, Chim. Int. J. Chem. 61 (2007) 355–360.
[3] T. Sehl, Z. Maugeri, D. Rother, J. Mol, Catal, B Enzym. 114 (2015) 65–71.
[4] E.D.D. Calder, A.M. Zaed, A. Sutherland, J. Org. Chem. 78 (2013) 7223–7233.
[5] O.N. Burchak, S. Py, Tetrahedron 65 (2009) 7333–7356.
[6] O.K. Karjalainen, A.M.P. Koskinen, Org. Biomol. Chem. 10 (2012) 4311–4326.
[7] M. Rahimi-Nasrabadi, S.M. Pourmortazavi, M.R. Ganjali, P. Norouzi, J. Mater. Sci. Mater. Electron. 28 (2017) 9724–9731.
[8] X. Miao, S. Wen, Y. Su, J. Fu, X. Luo, P. Wu, C. Cai, R. Jelinek, L.-P. Jiang, J.-J. Zhu, Anal. Chem. 91 (2019) 7295–7303.
[9] X. Shao, K. Li, S.J. Malcolmson, J. Am. Chem. Soc. 140 (2018) 7083–7087.
[10] K. Yabushita, A. Yuasa, K. Nagao, H. Ohmiya, J. Am. Chem. Soc. 141 (2019) 113–117.
[11] M. Takeda, A. Mitsui, K. Nagao, H. Ohmiya, J. Am. Chem. Soc. 141 (2019) 3664–3669.
[12] D.J. Pippel, G.A. Weisenburger, N.C. Faibish, P. Beak, J. Am. Chem. Soc. 123 (2001) 4919–4927.
[13] C. Gaul, D. Seebach, Helv. Chim. Acta 85 (2002) 963–978.
[14] S.L. Gargaro, R.K. Klake, K.L. Burns, S.O. Elele, S.L. Gentry, J.D. Sieber, Org. Lett. 21 (2019) 9753–9758.
[15] L. Ackermann, E. Diers, A. Manvar, Org. Lett. 14 (2012) 1154–1157.
[16] S. Matsunaga, M. Shibasaki, Chem. Commun. 50 (2014) 1044–1057.
[17] G. Blay, V. Hernández-Olmos, J.R. Pedro, Synlett 2011 (2011) 1195–1211.
[18] D.A. Evans, G.C. Andrews, Acc. Chem. Res. 7 (1974) 147–155.
[19] J.D. Zhang, J.W. Zhao, L.L. Gao, H.H. Chang, W.L. Wei, J.H. Xu, J. Biotechnol. 290 (2019) 24–32.
[20] F.F. Chen, S.C. Cosgrove, W.R. Birmingham, J. Mangas-Sanchez, J. Citoler, M.P. Thompson, G.W. Zheng, J.H. Xu, N.J. Turner, ACS Catal. 9 (2019) 11813–11818.
[21] I. Cho, C.K. Prier, Z.J. Jia, R.K. Zhang, T. Görbe, F.H. Arnold, Angew. Chemie - Int. Ed. 58 (2019) 3138–3142.
[22] C.Y. Huang, A.G. Doyle, Chem. Rev. 114 (2014) 8153–8198.
[23] E.N. Jacobsen, Acc. Chem. Res. 33 (2000) 421–431.
[24] J.A. Bodkin, M.D. McLeod, J. Chem, Soc. Perkin 24 (2002) 2733–2746.
[25] M.M. Heravi, T.B. Lashaki, B. Fattahi, V. Zadsirjan, RSC Adv. 8 (2018) 6634–6659.
[26] V.R. Yarapathy, S. Mekala, B.V. Rao, S. Tammishetti, Catal. Commun. 7 (2006) 466–471.
[27] I. Cepanec, M. Litvić, H. Mikuldaš, A. Bartolinčić, V. Vinković, Tetrahedron 59 (2003) 2435–2439.
[28] A.K. Chakraborti, S. Rudrawar, A. Kondaskara, European J, Org. Chem. 2004 (2004) 3597–3600.
[29] J.E. Chateauneuf, M.T.H. Liu, J. Org. Chem. 56 (1991) 5942–5943.
[30] M. Chini, P. Crotti, F. Macchia, Tetrahedron Lett. 31 (1990) 4661–4664.
[31] S. Rampalli, S.S. Chaudhari, K.G. Akamanchi, Synthesis (Stuttg). 2000 (01) (2000) 78–80.
[32] A.R. Khosropour, M.M. Khodaei, K. Ghozati, Chem. Lett. 33 (2004) 304–305.
[33] G.H. Posner, D.Z. Rogers, J. Am. Chem. Soc. 99 (1977) 8208–8214.
[34] H. Kotsuki, K. Hayashida, T. Shimanouchi, H. Nishizawa, J. Org. Chem. 61 (1996) 984–990.
[35] S. Roy, P. Bhanja, S.S. Islam, A. Bhaumik, S.M. Islam, Chem. Commun. 52 (2016) 1871–1874.
[36] S. Lv, K. Zhang, L. Zhu, D. Tang. *Anal. Chem.* 92 (2020) 1470–1476.
[37] R. Zeng, W. Wang, G. Cai, Z. Huang, J. Tao, D. Tang, C. Zhu. *Nano Energy* 74 (2020) 104931.
[38] R. Zeng, W. Wang, M. Chen, Q. Wan, C. Wang, D. Knopp, D. Tang. *Nano Energy* 82 (2021) 105711.
[39] H. Karimi-Maleh, Y. Orooji, A. Ayati, S. Qanbari, B. Tanhaei, F. Karimi, M. Alizadeh, J. Rouhi, L. Fu, M. Sillanpää, J. Mol. liquids (2020) 115062.
[40] H. Karimi-Maleh, B. Ganesh, K. Saravanan, R. Jiaqian, Q.S. Vadivel, D. Durgalakshmi, F. Graciaj, M. Soto-Moscosok, Y. Orooji, F. Karimi, J. Mol. liquids 314 (2020) 113588.
[41] H. Karimi-Maleh, F. Karimi, Y. Orooji, G. Mansouri, A. Razmjou, A. Aygun, F. Sen. *Sci. Report* 10 (2020) 11699.
[42] H. Karimi-Maleh, F. Karimi; S. Malekmohammadi; N. Zakariae, R. Esmaeili, S. Rostamnia, M. Lütfi Yola, N. Atar, S. Movagharnezhad, S. Rajendran, A. Razmjou, Y. Orooji, S. Agarwal, V. Kumar Gupta. *J. Mol. liquids.* 2020, 310, 113185.
[43] H. Karimi-Maleh, K. Cellat, K. Arıkan, A. Savk, F. Karimi, F. Şen. Mater. Chem. Physics 250 (2020) 123042.
[44] Y. Liu, Y. Zhou, S. Yu, Z. Xie, Y. Chen, K. Zheng, S. Mossin, W. Lin, J. Meng, T. Pullerits, K. Zheng, ACS Appl. Nano Mater. 3 (2020) 772–781.
[45] G. Cai, Z. Yu, P. Tong, D. Tang, Nanoscale 11 (2019) 15659–15667.
[46] J. Shu, D. Tang, Chem. Asian J. 12 (2017) 2780–2789.
[47] Z. Qiu, J. Shu, D. Tang. *Anal. Chem.* 89 (2017) 5152–5160.
[48] P. Li, C. Wu, Y. Xu, D. Cheng, Q. Lu, J. Gao, W. Yang, X. Zhu, M. Liu, H. Li, P. Yin, Y. Zhang, Trends Anal. Chem. 131 (**2020**) 116007.
[49] J. Deng, Q. Lu, Y. Hou, M. Liu, H. Li, Y. Zhang, *S. Yao. Anal. Chem.* 87 (2015) 2195–2203.
[50] X. Zhu, T. Zhao, Z. Nie, Y. Liu, *S. Yao. Anal. Chem.* 87 (2015) 8524–8530.
[51] S. Zhang, R. Li, X. Liu, L. Yang, Q. Lu, M. Liu, H. Li, Y. Zhang, S. Yao, Biosens. Bioelectron. 92 (2017) 457–464.
[52] Z. Ma, Y. Sun, J. Xie, P. Li, Q. Lu, M. Liu, P. Yin, H. Li, Zhang, *S, Yao. ACS Appl Mater Interfaces.* 12 (13) (2020) 15919–15927.
[53] S. Sangam, A. Gupta, A. Shakeel, R. Bhattacharya, A.K. Sharma, D. Suhag, S. Chakrabarti, S.K. Garg, S. Chattopadhyay, B. Basu, V. Kumar, S.K. Rajput, M.K. Dutta, M. Mukherjee, Green Chem. 20 (2018) 4245–4259.
[54] H. Rouh, Y. Liu, N. Katakam, L. Pham, Y.L. Zhu, G. Li, J. Org. Chem. 83 (2018) 15372–15379.
[55] B. Movassagh, H. Rooh, H.R. Bijanzadeh, Chem. Heterocycl. Compd. 48 (2013) 1719–1721.
[56] L.S. Li, X. Yan, J. Phys. Chem. Lett. 1 (2010) 2572–2576.

[57] C.X. Guo, H. Bin Yang, Z.M. Sheng, Z.S. Lu, Q.L. Song, C.M. Li, Angew. Chemie - Int. Ed. 49 (2010) 3014–3017.
[58] X. Yan, X. Cui, B. Li, L.S. Li, Nano Lett. 10 (2010) 1869–1873.
[59] X. Geng, L. Niu, Z. Xing, R. Song, G. Liu, M. Sun, G. Cheng, H. Zhong, Z. Liu, Z. Zhang, L. Sun, H. Xu, L. Lu, L. Liu, Adv. Mater. 22 (2010) 638–642.
[60] S. Zhu, J. Zhang, C. Qiao, S. Tang, Y. Li, W. Yuan, B. Li, L. Tian, F. Liu, R. Hu, H. Gao, H. Wei, H. Zhang, H. Sun, B. Yang, Chem. Commun. 47 (2011) 6858–6860.
[61] X.T. Zheng, A. Ananthanarayanan, K.Q. Luo, P. Chen, Small 11 (2015) 1620–1636.
[62] S.J. Jeon, T.W. Kang, J.M. Ju, M.J. Kim, J.H. Park, F. Raza, J. Han, H.R. Lee, J.H. Kim, Adv. Funct. Mater. 26 (2016) 8211–8219.
[63] D. Pan, J. Zhang, Z. Li, M. Wu, Adv. Mater. 22 (2010) 734–738.
[64] Z. Liu, J.T. Robinson, X. Sun, H. Dai, J. Am. Chem. Soc. 130 (2008) 10876–10877.
[65] S. Benítez-Martínez, Á.I. López-Lorente, M. Valcárcel, Anal. Chem. 86 (2014) 12279–12284.
[66] M.M. Vaidergorn, Z.A. Carneiro, C.D. Lopes, S. de Albuquerque, F.C.C. Reis, S. Nikolaou, J.F.R.E. Mello, G.L. Genesi, G.H.G. Trossini, A. Ganesan, F.S. Emery, Eur. J. Med. Chem. 157 (2018) 657–664.
[67] L. Mouls, G. Subra, C. Enjalbal, J. Martinez, J.L. Aubagnac, Tetrahedron Lett. 45 (2004) 1173–1178.
[68] D. Soto-Castro, R.C. Lara Contreras, M. Pina-Canseco, R. Santillán, M.T. Hernández-Huerta, G.E. Negrón Silva, E. Pérez-Campos, S. Rincón, Steroids 126 (2017) 92–100.
[69] X. Mu, J. Qiao, L. Qi, Y. Liu, H. Ma, ACS Appl, Mater. Interfaces 6 (2014) 12979–12987.
[70] J.L. Manzoori, M. Amjadi, J. Soleymani, E. Tamizi, A. Rezamand, A. Jouyban, Luminescence 27 (2012) 268–273.
[71] A. Jouyban, M. Shaghaghi, J.L. Manzoori, J. Soleymani, J. Jalilvaez-Gharamaleki, Iran. J. Pharm. Res. IJPR 10 (2011) 695–704.